

# Aspartate–Histidine Interaction in the Retinal Schiff Base Counterion of the Light-Driven Proton Pump of *Exiguobacterium sibiricum*

S. P. Balashov,<sup>\*,†</sup> L. E. Petrovskaya,<sup>\*,‡</sup> E. P. Lukashev,<sup>§</sup> E. S. Imasheva,<sup>†</sup> A. K. Dioumaev,<sup>†</sup> J. M. Wang,<sup>†</sup> S. V. Sychev,<sup>‡</sup> D. A. Dolgikh,<sup>‡,§</sup> A. B. Rubin,<sup>§</sup> M. P. Kirpichnikov,<sup>‡,§</sup> and J. K. Lanyi<sup>\*,†</sup>

<sup>†</sup>Department of Physiology and Biophysics, University of California, Irvine, California 92697, United States

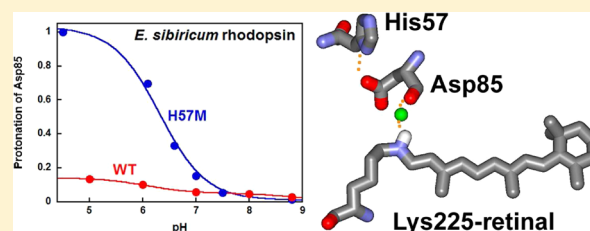
<sup>‡</sup>Shemyakin and Ovchinnikov Institute of Bioorganic Chemistry, Moscow 117997, Russia

<sup>§</sup>Department of Biology, Lomonosov Moscow State University, Moscow 119991, Russia

## S Supporting Information

**ABSTRACT:** One of the distinctive features of eubacterial retinal-based proton pumps, proteorhodopsins, xanthorhodopsin, and others, is hydrogen bonding of the key aspartate residue, the counterion to the retinal Schiff base, to a histidine. We describe properties of the recently found eubacterium proton pump from *Exiguobacterium sibiricum* (named ESR) expressed in *Escherichia coli*, especially features that depend on Asp–His interaction, the protonation state of the key aspartate, Asp85, and its ability to accept a proton from the Schiff base during the photocycle. Proton

pumping by liposomes and *E. coli* cells containing ESR occurs in a broad pH range above pH 4.5. Large light-induced pH changes indicate that ESR is a potent proton pump. Replacement of His57 with methionine or asparagine strongly affects the pH-dependent properties of ESR. In the H57M mutant, a dramatic decrease in the quantum yield of chromophore fluorescence emission and a 45 nm blue shift of the absorption maximum with an increase in the pH from 5 to 8 indicate deprotonation of the counterion with a  $pK_a$  of 6.3, which is also the  $pK_a$  at which the M intermediate is observed in the photocycle of the protein solubilized in detergent [dodecyl maltoside (DDM)]. This is in contrast with the case for the wild-type protein, for which the same experiments show that the major fraction of Asp85 is deprotonated at pH >3 and that it protonates only at low pH, with a  $pK_a$  of 2.3. The M intermediate in the wild-type photocycle accumulates only at high pH, with an apparent  $pK_a$  of 9, via deprotonation of a residue interacting with Asp85, presumably His57. In liposomes reconstituted with ESR, the  $pK_a$  values for M formation and spectral shifts are 2–3 pH units lower than in DDM. The distinctively different pH dependencies of the protonation of Asp85 and the accumulation of the M intermediate in the wild-type protein versus the H57M mutant indicate that there is strong Asp–His interaction, which substantially lowers the  $pK_a$  of Asp85 by stabilizing its deprotonated state.



*Exiguobacterium sibiricum* 255-15, a Gram-positive psychrophilic eubacterium, was isolated from a 43.6 m depth of a 2–3 million year old permafrost core.<sup>1,2</sup> Its genome contains a gene for a retinal protein termed ESR,<sup>3</sup> with homology to other proton pumps such as the archaeal bacteriorhodopsins,<sup>4–6</sup> the eubacterial proteorhodopsins,<sup>7</sup> and xanthorhodopsin.<sup>8,9</sup> Its amino acid sequence indicates that, as in the other pumps, in ESR the key component of the counterion to the Schiff base and probable proton acceptor is a conserved aspartate, Asp85, homologous to Asp85 of bacteriorhodopsin.<sup>10</sup> As in the eubacterial proton pumps, proteorhodopsin,<sup>11,12</sup> xanthorhodopsin,<sup>13</sup> and the more recently described *Gloeobacter* rhodopsin,<sup>14</sup> but not in bacteriorhodopsin, there is a histidine residue (His57) that might interact closely with Asp85. The only other positively charged residue in this region is Arg82. A unique and intriguing difference from all other known pumps is that in the cytoplasmic domain Lys96 takes the place of the internal proton donor to the Schiff base, Asp96 in bacteriorhodopsin<sup>15–17</sup> and the homologous glutamic acid in other eubacterial pumps.<sup>13,18</sup>

The ESR gene was expressed in *Escherichia coli*, and upon incubation with all-*trans*-retinal, the protein formed a chromophore with an absorption maximum at 534 nm.<sup>3</sup> Proteoliposomes containing ESR produced light-induced acidification, confirming its ability to conduct light-induced proton transport.<sup>3</sup> In spite of the absence of the usual carboxylic residue as the internal proton donor, the turnover of the ESR photocycle is comparable to those in proteorhodopsin<sup>18,19</sup> and xanthorhodopsin.<sup>8,20</sup>

In this paper, we extend characterization of this novel proton pump, focusing on features that depend on the Schiff base counterion Asp85 and especially on the possible Asp–His interaction. A strong hydrogen bond between the imidazole ring and the carboxylate of the two homologous residues was found in the crystallographic structure of xanthorhodopsin.<sup>13</sup> The role of His in the counterion complex was the subject of

Received: March 31, 2012

Revised: June 26, 2012

Published: June 27, 2012



several studies on proteorhodopsin also, using homology modeling,<sup>11</sup> mutagenesis,<sup>12,21</sup> FTIR,<sup>12</sup> and NMR.<sup>21</sup> In this study of ESR, we address several related questions. (i) What is the pH range of the functional activity of ESR as a proton pump and the  $pK_a$  of the counterion? (ii) Is there a significant effect of replacing His57 and Arg82 with uncharged residues? (iii) How does His57 influence the  $pK_a$  of Asp85? (iv) Is there coupling of the protonation states of these residues? (v) How do changes in the protonation state of the counterion correlate with events in the photocycle? (vi) What are the kinetics of proton release and uptake during the photocycle and their connection to the other photocycle reactions? The role of Lys96 in reprotonation of the Schiff base in ESR will be examined in a separate study.

## MATERIALS AND METHODS

ESR was expressed in *E. coli* and purified as described previously.<sup>3</sup> Typically, the protein was solubilized in 0.1–0.2% DDM. Samples contained 100 mM NaCl and several buffers (citric acid, MES, MOPS, HEPES, CHES, and CAPS), at 5 mM each. ESR mutants, D85N, R82Q, H57M, H57N, H57R, and K96A, were produced as follows. Mutant genes were constructed using two-step SOE-PCR<sup>22</sup> with *Pfu* DNA polymerase (Fermentas) using the wild-type ESR gene in the pET-ESR plasmid as a template. Mutagenic primers were as follows: K96A\_for, ctgttgctagctgctttccattgttgc; K96A\_rev, gcaacaatggaagcgactagcaacag; D85N\_for, ccgttatatcaattggctcgtcacgac; D85N\_rev, gtgacgagccaattgatatacggatttc; R82Q\_for, acagaaatccagtatatcgactggctcgtcac; R82Q\_rev, agtcgataactggatttctgttgaaacgc; H57M\_for, gccattatgtattcttatgaaagatgc; H57M\_rev, cataaagtaatacataatggcgcgcgacaaagg; H57KRNS\_for, gccattarmtattactttatgaaagatgc; H57KRNS\_rev, cataaagtaatakytaatggcgcgcgacaaagg (the last pair enabled construction of 4 mutations of H57 in parallel). T7prom and T7rev standard primers used as flanking primers were synthesized by Evrogen (Moscow, Russia). The resulting products were cloned into the pET32a vector as described in ref 3. Mutations were confirmed by DNA sequencing (Genome Centre, Moscow, Russia). Purification of the mutant proteins was as described for wild-type ESR.<sup>3</sup> It involved binding of the solubilized six-His-tagged proteins to a Ni column and elution with imidazole buffer. To determine whether the six-His tag affects any properties of the protein, a standard thrombin cleavage site (LeuValProArgGlySer) was engineered into the C-terminus, which allowed the removal of the six-His tag, as verified with gel electrophoresis (Figure S1 of the Supporting Information). A control experiment on a protein without a six-His tag revealed no substantial effect on the pH dependence of M formation [the  $pK_a$  was increased by ~0.5 unit, so that the amount of M at pH 9 was similar to that at pH 8.5 when the six-His tag was present (see Figure S2 of the Supporting Information)]. In all other experiments, six-His-tagged proteins were used. Protein solubilized in DDM was used in most experiments, except in cases where it is explicitly stated that another detergent, LPG (Avanti Polar Lipids Inc., catalog no. 858122), or *E. coli* cells with ESR expressed or proteoliposomes were used.

**Proteoliposomes Containing ESR for Measurements of Light-Induced pH Changes.** These proteoliposomes were prepared using soybean phosphatidylcholine from Lipoid, type S-100, and TLC grade as described in ref 23. The protein:lipid molar ratio was 1:1700. The diameter of liposomes was  $60 \pm 5$  nm as determined by dynamic light scattering on a Coulter N4MD submicrometer particle analyzer. A 100  $\mu$ L proteolipo-

some suspension (protein concentration of 0.25 mg/mL) was added to 2 mL of a 0.75 M NaCl solution in Milli-Q water (Millipore). Measurements were taken in the thermostated cell at 25 °C with rapid stirring. The pH was monitored with the Radiometer PHM82 pH-meter and Cole-Parmer RZ-05658-65 electrode shielded from radiation. Samples were illuminated with a 500 W halogen lamp (OSRAM) from a distance of 35 cm. Light passed through a cutoff filter transmitting at  $\lambda > 480$  nm and a filter cutting off the infrared portion of the spectrum to avoid heating.

**Proteoliposomes for the Time-Resolved Spectroscopic Measurements.** These proteoliposomes were prepared at a 1:100 protein:lipid molar ratio with L- $\alpha$ -phosphatidylcholine (Avanti Inc., catalog no. 840051C). The high protein/lipid ratio in these samples was used to make them suitable for parallel FTIR studies.

**Measurements of Light-Induced pH Changes in Suspensions of *E. coli* Cells That Contained ESR.** These measurements were taken in a 1 cm  $\times$  1 cm cuvette with a stirrer as described previously.<sup>8</sup> The cells were carefully washed from buffers and organic components of cultivation media and resuspended in a 10 mM NaCl/10 mM MgCl<sub>2</sub>/2.5 mM KCl solution. Illumination was at 480–650 nm using a light intensity below the saturating level. All-trans-retinal for reconstitution of ESR and the protonophore CCCP were from Sigma-Aldrich. The polar lipids of *E. sibiricum*<sup>2</sup> are composed of phosphatidylglycerol, phosphatidylethanolamine, and diphosphatidylglycerol. The first two are present in *E. coli*,<sup>24</sup> so one can expect that ESR expressed in *E. coli* should be in environment closer to native than in detergents and liposomes, and that this would help to establish the physiological pH range of ESR proton pumping capability. Previously, light-induced pH changes were detected similarly, in suspensions of *E. coli* cells containing proteorhodopsin.<sup>25</sup>

**Spectral and Kinetic Measurements of Solubilized ESR and Proteoliposomes.** All measurements were taken at 22 °C. Absorption spectra were measured on a Shimadzu UV1700 spectrophotometer. The pH in the cuvette was measured with a micro pH electrode (VanLondon pHoenix, Houston, TX). Fluorescence emission and fluorescence excitation spectra were recorded on an Aminco-SLM instrument in 5 mm  $\times$  5 mm quartz cells (Starna cells, Inc.) as described previously.<sup>26</sup> The kinetics of laser-induced absorption changes in the 2  $\mu$ s to 10 s time domain were obtained on the single-wavelength kinetic system as described previously,<sup>20</sup> using 7 ns, 532 nm flashes for photoexcitation from a Nd:YAG laser. The excitation intensity was  $< 3$  mJ/cm<sup>2</sup> to prevent degradation of the chromophore.<sup>27</sup> One hundred or more traces were averaged to achieve a higher signal-to-noise ratio. The duration between flashes was set to be in the range between 1 and 20 s to allow completion of a photocycle. The kinetic traces were fit with FitExp.<sup>28</sup> Time-resolved difference spectra of light-induced absorption changes (in the 200 ns to seconds time domain) were collected on an Optical Multichannel Analyzer (OMA) built on a Shamrock 303i spectrometer with an iStar ICCD sensor (Andor Technology).

**Kinetics of Light-Induced Proton Uptake and Release.** Transient proton release and uptake during the photocycle of ESR solubilized in detergent were followed by measuring absorption changes of the pH sensitive dye pyranine at 456 nm, as in analogous studies of bacteriorhodopsin<sup>29</sup> and proteorhodopsin.<sup>18</sup> The measurements were taken in a 5 mm  $\times$  5 mm cell. The concentrations of the dye and ESR were ~100 and

~10  $\mu$ M, respectively. In 0.2% DDM and 100 mM NaCl, the  $pK_a$  of the dye was 7.2. The measurements were taken at a pH close to the  $pK_a$  of the dye for the highest sensitivity. The dye response was determined as the difference between two traces of flash-induced absorption changes at 456 nm: that after addition of the dye minus that before addition (0.5  $\mu$ L was added to a 500  $\mu$ L ESR solution). To verify that the dye response can be quenched with a buffer and hence originates from transient light-induced proton concentration changes, a third trace was obtained after addition of a small volume of buffer (2–3  $\mu$ L to make the final concentration 5 mM). Stock solutions of 0.5 M MOPS or HEPES with a pH adjusted to the pH of a sample were used.

## RESULTS

**pH Dependence of the Retinal Chromophore Absorption Band of ESR and Its Relationship to the Protonation of the Counterion.** The absorption maximum of the wild-type protein is 534 nm at pH 5; it shifts to 521 nm at pH 10.5 (Figure 1A). The full pH dependence of the absorption maximum is described by a complex titration curve (Figure 1B), in which there are three transitions involving blue shifts: from 545 to ~534 nm with an apparent  $pK_a$  of 2.3, a second transition of an additional blue shift of 3 nm with an apparent  $pK_a$  of 6, and a third transition with a further blue shift of 10 nm with an apparent  $pK_a$  of ~9. The difference spectra of the latter two transitions are not the same, as they exhibit minima at 577 and 553 nm, respectively (Figure 1C). Characteristic blue shifts of the absorption maxima of microbial retinal proteins are associated with deprotonation of the aspartate that interacts with the Schiff base, as a principal part of its counterion and proton acceptor during the photocycle, e.g., Asp85 in bacteriorhodopsin,<sup>30</sup> Asp97 in green-absorbing proteorhodopsin,<sup>18,19</sup> and Asp96 in xanthorhodopsin.<sup>20</sup> The question is whether any of the transitions in the ESR spectrum in Figure 1 can be assigned to protonation of the counterion. Full neutralization of the negative charge on Asp85 in the ESR D85N mutant produced a pigment with a maximum at 563 nm at pH 5 (Figure 1A). This comprises a 29 nm red shift compared to the maximum at pH 5 and a 42 nm red shift relative to the maximum at pH 10.5 in the wild-type ESR. The much shorter wavelength of the maximum of the wild-type protein and the much smaller shift in the maximum (Figure 1B) suggest that only a minor fraction of Asp85 might be protonated at pH >3, and no more than partial protonation takes place even at pH 2. The retinal fluorescence spectra (see below) confirm this interpretation. A detailed study at pH <2 was not possible because the protein becomes unstable in this pH range.

**Effects of the R82Q, R82H, H57M, and H57N Mutations on the Chromophore Absorption Band and the  $pK_a$  of the Counterion.** The complex titration and partial protonation of the counterion might be due to interaction of Asp85 with other charged or ionizable groups. An example would be the interaction of Asp85 with Arg82 and other components of the proton release complex in bacteriorhodopsin.<sup>31,32</sup> Surprisingly, in ESR, the R82Q mutation did not produce any significant effect on the absorption maximum or the pH dependence of the absorption maximum when compared to that of the wild type (Figure 2A). Similar results were obtained for the R82H mutant (not shown). Such weak coupling of the corresponding arginine with the counterion was described also for proteorhodopsin.<sup>33</sup>

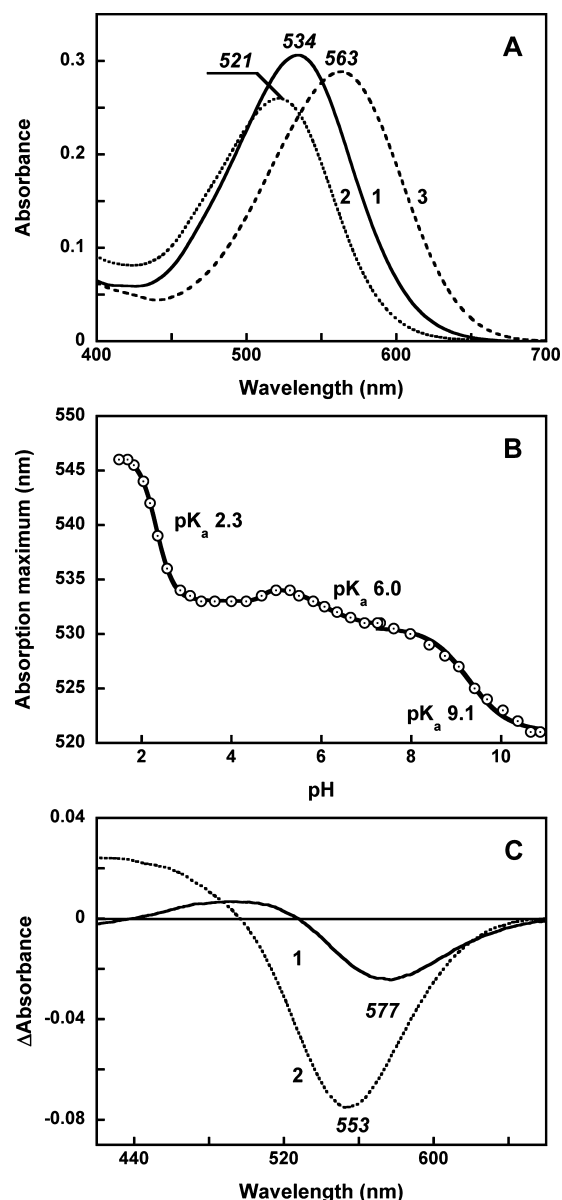


**Figure 1.** pH dependence of the retinal chromophore absorption band of ESR and the effect of the D85N mutation. (A) Wild-type ESR at pH 5 (1), wild-type ESR at pH 10.5, (2), and D85N mutant at pH 5 (3). (B) pH dependence of absorption maximum of ESR. All spectra were recorded in 0.2% DDM and 0.1 M NaCl. (C) Difference spectra of pH-induced absorption changes in ESR: (1) pH 7 minus pH 5 and (2) pH 10 minus pH 7.

The other possible candidate for interaction with Asp85 is His57, as the crystallographic structure of xanthorhodopsin<sup>13</sup> and mutagenesis of this residue in proteorhodopsin<sup>12,21</sup> suggest. Replacement of the histidine with methionine (the homologous residue in bacteriorhodopsin) causes dramatic changes in the pH dependence of the absorption maximum and in other properties of the protein. We find that at pH 5 the maximum is now at 565 nm, close to that in the D85N mutant, suggesting that unlike in the wild type, there is complete protonation of Asp85 (Figure 2A). When the pH is increased to 8.5, the maximum undergoes a large, 47 nm, blue shift, to 517 nm, in a single transition with a  $pK_a$  of 6.3, which is characterized by a difference spectrum with a maximum at 582 nm (Figure 2B). An additional 4 nm shift to 513 nm occurs



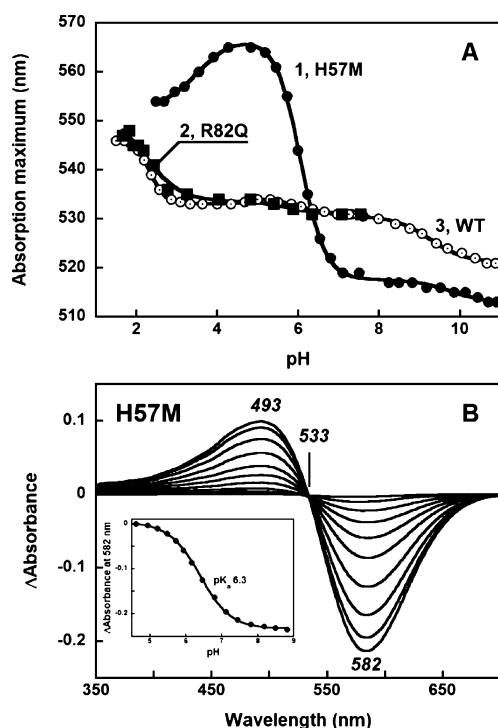


**Figure 2.** pH-dependent transitions in the absorption band of the H57M and R82Q mutants in comparison with those of the wild type. (A) Absorption maximum vs pH in (1) H57M, (2) R82Q, and (3) the wild type. (B) Difference spectra when the pH is increased from 4.5 to 7.4 from deprotonation of the counterion with a  $pK_a$  of 6.3 (see the inset) in the H57M mutant (the “pH<sub>i</sub> – pH 4.5” spectra were obtained at pH<sub>i</sub> values of 4.9, 5.2, 5.5, 5.7, 5.9, 6.2, 6.5, 6.8, 7.1, and 7.4).

when the pH is increased from 9 to 10.5 (Figure 2A). A similar phenotype is produced by the H57N mutation (not shown). We assign the major spectral transition with a  $pK_a$  of 6.3 in H57M to protonation of Asp85. The difference in the pH dependence of the absorption spectrum of the wild type versus the His57-substituted mutants implies that there is strong interaction between Asp85 and His57, and in the wild type, this interaction results in only partial protonation of Asp85 over a broad pH range. At pH <4.5, the absorption maximum of H57M undergoes a blue shift (Figure 2A). Its origin is unclear, but such partial reversal of the blue shift at acidic pH is a property of bacteriorhodopsin also,<sup>34,35</sup> where it is caused by binding of a chloride ion near the protonated counterion.

In the H57M mutant, the 10 nm blue shift with a  $pK_a$  of 9 observed in the wild type is absent, although a smaller shift (4 nm) occurs at higher pH values. The difference spectrum of this transition (maximum at 562 nm) is different from the absorption changes associated with protonation of the counterion at pH <7 (maximum at 582 nm), indicating that it is not caused by a change in the protonation of Asp85.

**Estimation of the Fraction of the Protonated Counterion from Fluorescence Excitation Spectra.** The fluorescence of the retinal chromophore is an independent assay for the protonation state of the counterion. In bacteriorhodopsin, the lifetime of the excited state, and therefore the fluorescence intensity, increases by more than 1 order of magnitude upon protonation of the counterion at low pH or its neutralization by the D85N mutation.<sup>36–38</sup> A similar increase in the lifetime of the excited state was observed also for proteorhodopsin upon protonation of the counterion<sup>39</sup> or its neutralization by

mutation.<sup>40</sup> To quantify the fraction of protonated Asp85 and to determine whether the observed 10 nm blue shift with a  $pK_a$  of 9 in the wild type can be caused by protonation of the counterion, we examined the pH dependence of fluorescence from the retinal chromophore in wild-type ESR and compared it to that of the D85N and H57M mutants.

The fluorescence emission of the D85N mutant of ESR, with a maximum at 686 nm, is several-fold more intense than that of the wild-type protein at pH 7 and 5 (Figure 3A). In the mutant, the excitation spectrum (maximum at 564 nm) virtually coincides with the maximum of the absorption band (maximum at 563 nm), indicating that the emission is from the majority of the D85N pigment (Figure 3B). In contrast, in the wild type, the excitation spectrum at pH 7 is 25 nm red-shifted from the absorption spectrum (556 nm vs 531 nm) (shown in Figure 3C with normalized amplitudes). This indicates that at pH 7 the emission originates mostly from a minor component that does not significantly contribute to the absorption spectrum but dominates the excitation spectrum. This is consistent with the observed much lower emission intensity of the wild type compared to that of D85N (Figure 3A). Assuming that the excitation spectrum can be deconvoluted into two components, one with a maximum at 564 nm (intense fluorescence from a fraction of the pigment with a protonated counterion) and another with a maximum at 531 nm (weak fluorescence from deprotonated species), we estimate that the amplitude of the first component in the wild type is ~12 times smaller than in the D85N mutant. From this, the fraction of the pigment with a protonated counterion can be estimated to be ~8% at pH 7.

When the pH is lowered from 7 to 5, the intensity of the fluorescence of wild-type ESR at 720 nm is increased 2-fold, and the maximum of the excitation spectrum shifts to 565 nm, indicating the increase in the fraction of the pigment with a protonated counterion. When the pH is increased from 7 to 8.8, the fluorescence intensity decreases and the maximum in the excitation spectrum shifts to 538 nm (closer to the unprotonated chromophore absorption maximum at 528 nm), indicating a decrease in the fraction of protonated Asp85 (Figure 3D). A simple way of estimating the fraction of protonated species, without deconvolution of the spectra, is from the amplitude of the excitation spectrum at wavelengths of >610 nm, where the contribution from the absorption (and therefore emission) of the pigment with an unprotonated counterion is negligibly small. The excitation spectrum of H57M at pH 5 was used as the reference for the fully protonated counterion. In Figure 3E, the fluorescence intensity for excitation at 610 nm in the wild type and the H57M mutant (measured under identical conditions) is plotted on a log scale. Curve 1 in Figure 3E, thus, represents the pH dependence of the fraction of protonated Asp85 in wild-type ESR, which remains low between pH 5 and 10, in agreement with the data on the shift in the absorption maxima (see above). The protonated fraction decreases from ~15% at pH 5 to ~8% at pH 7 with a  $pK_a$  of 6 and decreases further to <5% with a  $pK_a$  of ~9.

Unlike in the wild type, in the H57M mutant the large blue shift of the absorption maximum that occurs with a  $pK_a$  of 6.3 (Figure 2B) fully correlates with dramatic changes in the fluorescence emission intensity with a similar  $pK_a$  and is accompanied by a shift in the emission maximum from ~690 nm at pH 4.5 to ~650 nm at pH 7.5 (Figure S3 of the Supporting Information). Corresponding changes occur in the excitation spectra (Figure 3F). When the pH is increased from

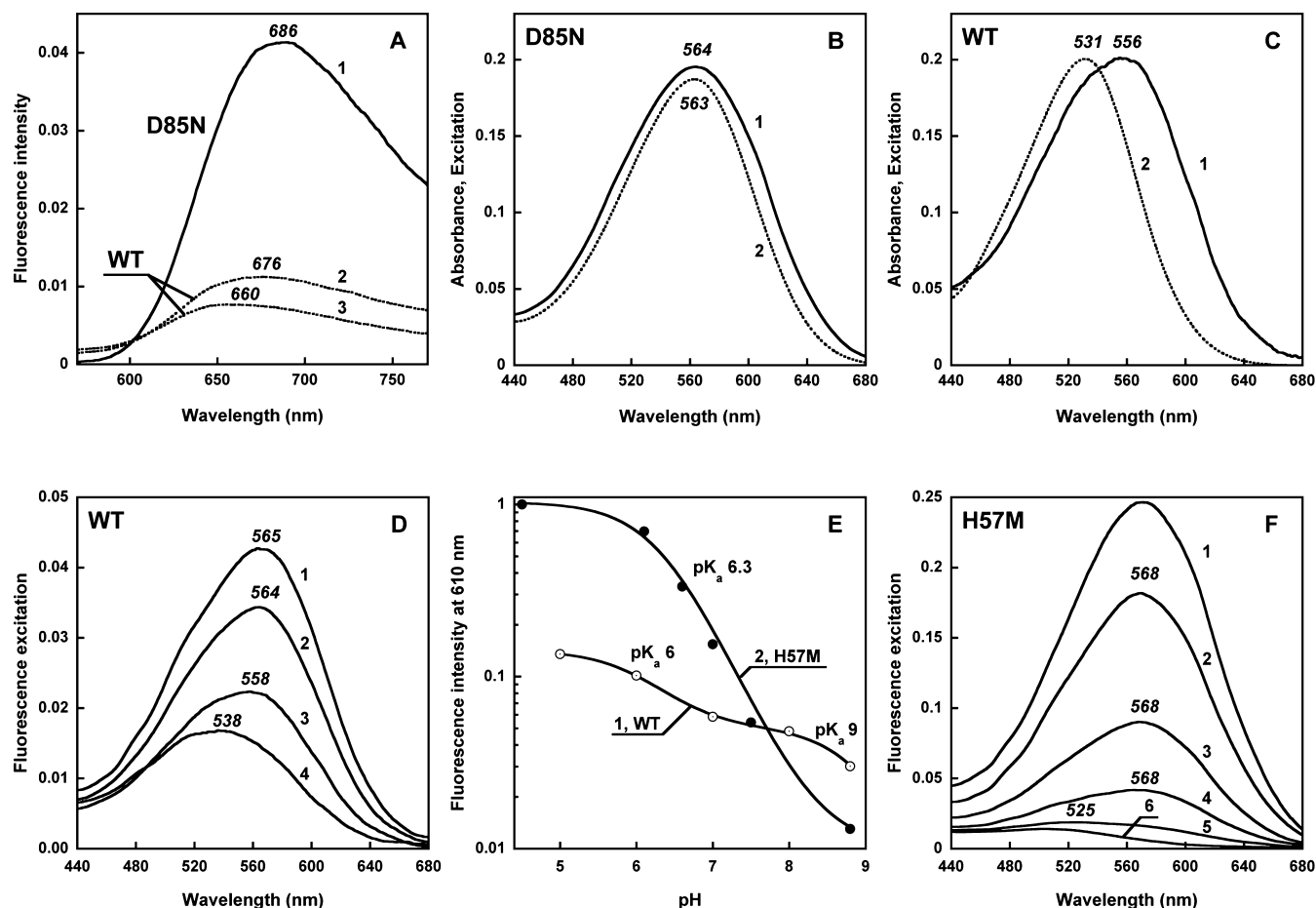


**Figure 3.** Fluorescence emission, excitation, and absorption spectra of wild-type ESR and the D85N and H57M mutants as a tool for estimating the fraction of the pigment with a protonated counterion. (A) Retinal chromophore fluorescence band measured under 530 nm excitation: (1) D85N mutant of ESR at pH 5, (2) wild type at pH 5, and (3) wild type at pH 7. The concentration of retinal proteins was 8  $\mu$ M. (B and C) Comparison of excitation (1) and absorption (2) spectra of D85N (B) and the wild type (C). (D) Fluorescence excitation spectra for the 720 nm emission of wild-type ESR at (1) pH 5, (2) pH 6, (3) pH 7, and (4) pH 8.8. (E) pH dependence of the fluorescence excitation spectrum at 610 nm, proportional to the fraction of protonated counterion: (1) wild-type ESR and (2) H57M. The amplitude of the spectrum at 610 nm in H57M at pH 4.5 was taken to be 1. (F) Fluorescence excitation spectra for the 720 nm emission of the H57M mutant at several pH values: pH 4.5, 6.1, 6.7, 7.0, 7.5, and 8.8 (1–6, respectively).

4.5 to 9, the excitation efficiency at 610 nm decreases almost 100-fold, with a  $pK_a$  of 6.3, clearly from the decrease in the fraction of protonated Asp85 (Figure 3E, curve 2). The excitation spectra for 720 nm emission undergo a similar decrease in amplitude with an increase in pH and exhibit a strong blue shift from  $\sim$ 568 nm at pH 4.5 to  $\sim$ 520 nm at pH 8.8 (Figure 3F).

**pH Dependence of the Photocycle of ESR: Accumulation of the M Intermediate.** An unexpected finding is that in spite of Asp85 being mostly unprotonated at pH  $>$ 3 (see above), the deprotonation of the retinal Schiff base in the photocycle of ESR solubilized in detergent, i.e., the accumulation of the M intermediate, is strongly pH-dependent above this pH. At pH 7.3, flash photoexcitation results first in the formation of a red-shifted intermediate analogous to the K state of bacteriorhodopsin.<sup>41</sup> It is characterized by a maximum at 590 nm and an isosbestic point at 548 nm (see the difference spectrum between the photoproduct and the initial state at a 200 ns delay after the flash in Figure 4A). During the first 10  $\mu$ s in the photocycle, there is a transition in which K is partly converted to another state with a maximum at shorter wavelengths, at 520–530 nm, which could be a shunt to the

initial ESR or more probably the production of an L-like state, using nomenclature from bacteriorhodopsin (Figure 4A). The kinetics of the change in absorption at 590 nm (Figure 5A) also reflects partial decay of the initial red-shifted photoproduct on the 10  $\mu$ s time scale. This is followed by a second red-shifted intermediate that persists until the end of the photocycle, decaying on a time scale of 100 ms (Figures 4B and 5A). Very little M is observed at neutral pH, as indicated also by single-wavelength measurement of the time dependence of the absorption change at 410 nm (Figure 5A).

The pattern is very different at pH  $\geq$ 9. The decay of the red-shifted K-like state becomes more complete and very rapid, and at pH 9.1, the M intermediate with a maximum at 400 nm appears within a few microseconds (Figures 4C and 5B). Its accumulation continues in the millisecond time domain where it reaches a maximal amplitude  $\sim$ 4 ms after a flash (Figures 4C and 5B). Formation of M at that time occurs from an intermediate with a maximum at  $\sim$ 515–520 nm (see the difference spectrum between traces taken at 2 ms and 100  $\mu$ s in Figure 4C), which is an L-like state as confirmed by FTIR (data not shown). The decay of M produces a red-shifted species with a difference maximum at 595 nm (Figure 4D) that

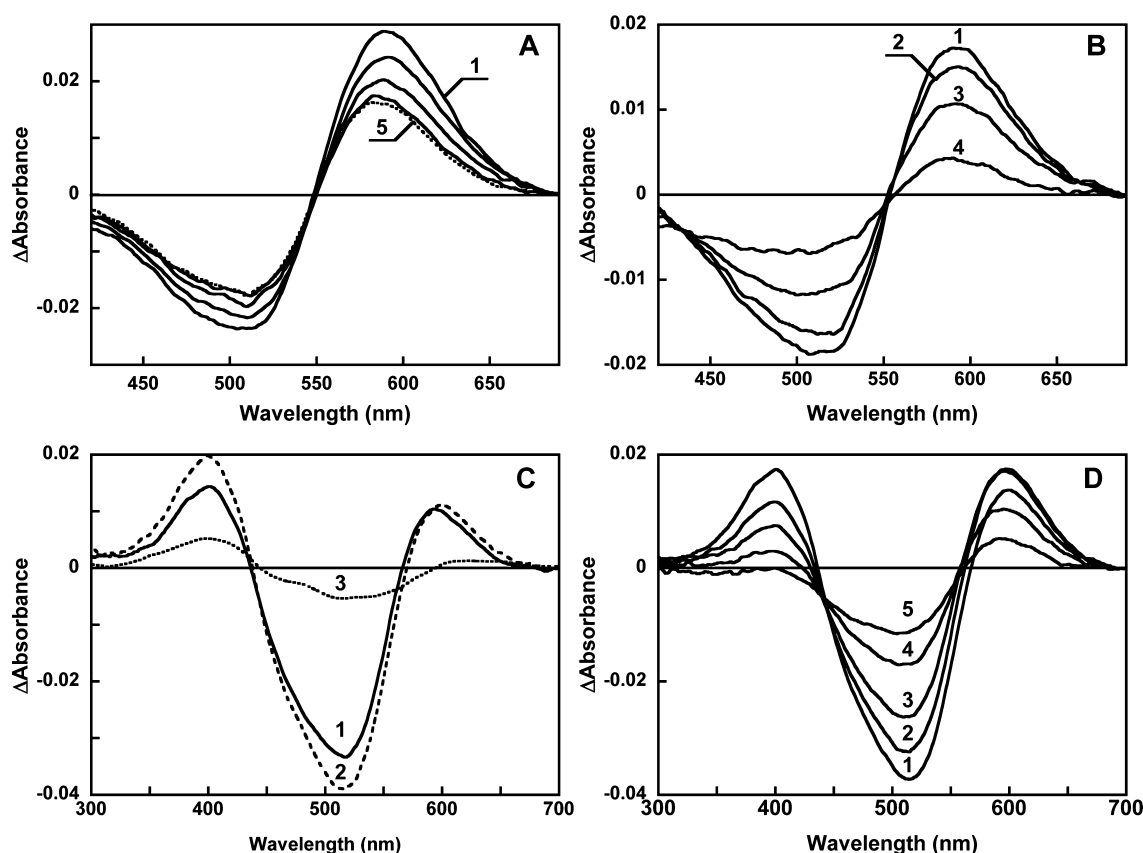


**Figure 4.** Absorption changes induced by a 532 nm laser flash in ESR at pH 7.3 (A and B) and pH 9.1 (C and D). (A) Spectra taken 0.2, 1, 2, 5, and 20  $\mu$ s after the flash (1–5, respectively). (B) Spectra taken 10, 20, 50, and 100 ms after the flash (1–4, respectively). (C) Spectra taken at 100  $\mu$ s (1) and 2 ms (2) and difference between spectra taken at 2 ms and 100  $\mu$ s (3). (D) Spectra taken 5, 10, 20, 50, and 100 ms after the flash (1–5, respectively).

indicates reprotonation of the Schiff base and protonation of the counterion and appears to be analogous to the mixture of N and O intermediates in the bacteriorhodopsin photocycle,<sup>41</sup> and apparently similar intermediate(s) in the photocycle of proteorhodopsin.<sup>18</sup>

Figure 5 contains measurements of time-dependent absorption changes in the photocycle at three pH values and four characteristic wavelengths, 590 nm for K and other red-shifted intermediate(s), 550 and 510 nm for initial state depletion and L formation, respectively, and 410 nm that assays mostly the M intermediate. At pH 7.6, the red-shifted photoproducts dominate at all times as indicated by the 590 nm trace (Figure 5A). The last of the red-shifted photoproducts decays with a time constant of  $\sim 90$  ms. As described above, at low and neutral pH, at pH  $\leq 7.6$ , the amount of observed M is very small, but at pH 9.1 and 9.8, it accumulates in large amounts. M rise (the trace at 410 nm) contains three components, and the rapid one, with a  $\tau_1$  of  $\sim 2$ –3  $\mu$ s, is followed by two slower components ( $\tau_2 \sim 30$   $\mu$ s, and  $\tau_3 \sim 2$ –3 ms). M rise, especially the components with  $\tau_1$  and  $\tau_3$  time constants, correlates with the decrease in the absorption at 590 nm from K conversion; the transition of the latter apparently involves the L-like intermediate, as follows from the large decrease in absorbance at 510 and 550 nm coincident with the rise of M (K to L to M). The decay of the M intermediate, which represents reprotonation of the Schiff base, involves at least two major components (13 and 67 ms, at pH 9.1). The first component correlates with the formation of the late red-shifted species.

The data show therefore that with an increase in pH from 7 to 10 a transition between two kinds of photocycles takes place, from one with very little M at neutral pH to another where the M intermediate and subsequent red-shifted state(s) dominate at pH  $> 9$ . As shown below, however, the absence of accumulation at pH  $< 9$  does not necessarily imply that M is not produced.

The transient accumulation of M increases with an apparent  $pK_a$  of  $\sim 8.8$ –9 (Figure 6). The  $pK_a$  of M yield is thus near the  $pK_a$  of one of the three blue shifts of the absorption maximum (Figure 1B). It is likely that the 10 nm blue shift and the appearance of M in the photocycle are related. In bacteriorhodopsin, deprotonation of Asp85 at pH  $> 2$  causes both a large (40 nm) blue shift of the absorption maximum and the appearance of the M intermediate because the proton acceptor is thereby made available.<sup>42</sup> In ESR, however, at pH 7, i.e., well below pH 9,  $\sim 90\%$  of Asp85 is unprotonated. Deprotonation of the rest, 8–10%, between pH 7 and 10 cannot be the cause of the observed dramatic increase in the yield of M in this pH range. Rather, both phenomena may be caused by deprotonation of another residue that affects the proton affinity of Asp85. An example of such a relationship is the coupling of proton affinity of Asp85 in bacteriorhodopsin to proton release complex and primarily to the conformation of Arg82. Substitution of the latter with a neutral residue causes a dramatic increase in the  $pK_a$  of Asp85 from 2.6 to 7.2 and accelerates M formation by 3 orders of magnitude.<sup>31</sup> Acceleration of M formation occurs also in bacteriorhodopsin at high pH, from deprotonation of the proton release

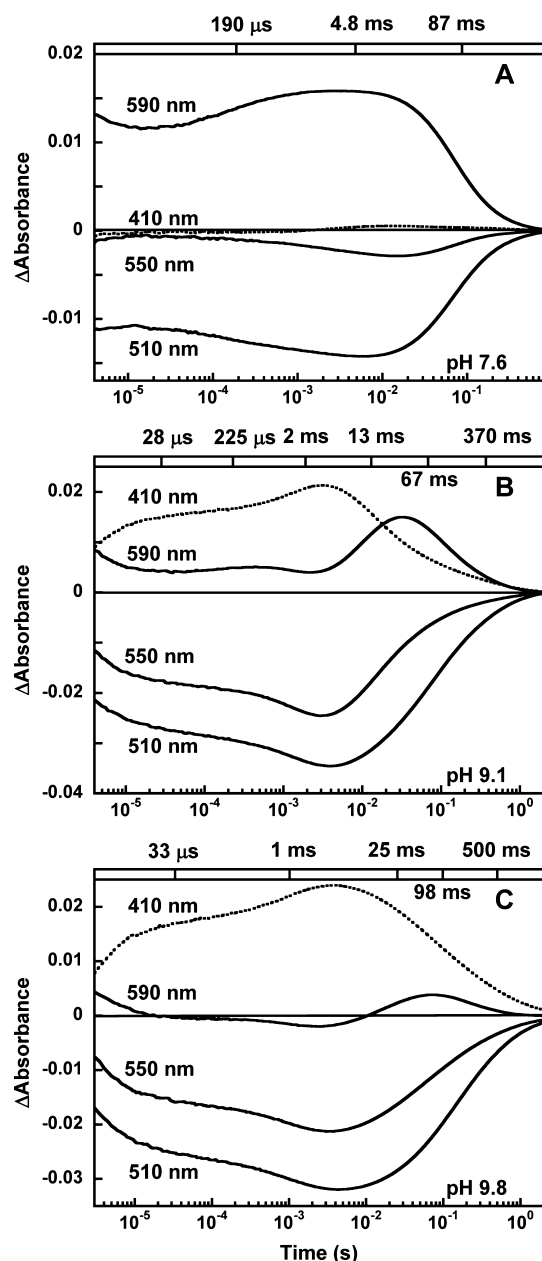


**Figure 5.** Kinetics of light-induced absorption changes of wild-type ESR at 410, 510, 550, and 590 nm at three pH values. The bars and numbers atop the panels represent the kinetic components that were determined from the global fit of absorption changes at the four wavelengths.

group.<sup>29,43</sup> In search for a potential candidate that can strongly influence the  $pK_a$  of Asp85 in ESR, and therefore possibly the accumulation of M, we examined the effects of replacing Arg82 and His57, the two residues that can contribute a positive charge in this region, on M formation.

**Effects of R82Q, H57M, and H57R Mutations on the Photocycle of ESR.** Unlike in the wild type, in the R82Q mutant very little of the M intermediate accumulates even at pH 9, as shown by the kinetic trace at 410 nm (Figure 7A). Thus, the effect of the substitution of Arg82 with an uncharged residue produces changes that are different from those described for bacteriorhodopsin: instead of acceleration of M formation, a strong decrease in the yield of M is observed. If Arg82 were the residue that was deprotonated with a  $pK_a$  of ~9

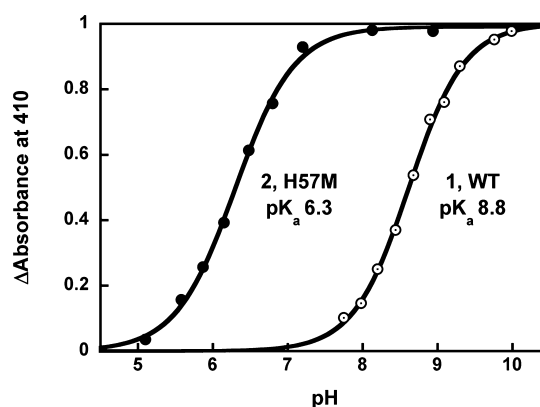


**Figure 6.** pH dependence of the yield of the M intermediate (normalized): (1) wild-type ESR and (2) H57M.

in the wild type, the consequence of the R82Q mutation would be an increased level of accumulation of M rather than a decreased one (Figure 7), and hence, deprotonation of Arg82 cannot be responsible for the appearance of M at high pH. The lack of accumulation of M at pH 9 in the mutant is a puzzle and implies a role for Arg82 in Schiff base deprotonation. The absorption maximum of the R82Q mutant at pH 9 is at 531 nm, which suggests a mostly unprotonated state for Asp85, and hence, it could accept a proton from the Schiff base provided that the  $pK_a$  difference is favorable and the path for the proton is available. Experiments with R82Q at pH >9 were not possible because the chromophore became unstable.

The H57M mutation has a great impact on the pH dependence of the yield of the M intermediate and on the kinetics of the photocycle (Figures 6 and 7B), but in a manner different from that of the Arg82 mutation. The M intermediate is observed at a pH lower than that of the wild type, well below 8 (Figure 7B). Its amplitude increases with a  $pK_a$  of 6.3 (Figure 6), coincident with the large blue shift of the absorption spectrum from deprotonation of Asp85 (Figure 2).

The kinetics of M rise in the H57M mutant is pH-independent, unlike in the wild type, and includes components with time constants of ~3 and ~30  $\mu$ s and a minor ~1 ms component seen at high pH where M decay is slower (not shown). At pH 7.7, it is biphasic (50% at 1.4 ms and 50% at 6 ms). The decay of M is accompanied by an increase in absorbance at 590 nm, which decays with time constants of 27 and 128 ms.

Substitution of His57 with arginine eliminates the accumulation of M between pH 6 and 9 (see Figure 4 of the Supporting Information) and eliminates the blue shift of the absorption spectrum with a  $pK_a$  of 9. The lack of M formation is similar to that of the homologous mutant of proteorhodopsin for which no protonation of Asp85 in the initial state and no M formation were observed.<sup>12</sup> This suggests that a positive charge placed at the His57 site interferes with light-induced deprotonation of the Schiff base, consistent with the interpretation of the results with ESR that His57, when protonated below pH 9, eliminates accumulation of M.

**Effect of the K96A Mutation on the Accumulation of M.** The kinetics of M formation in ESR contains relatively slow phases, in the millisecond time domain, in addition to the much more rapid phases. Their amplitude might be masked by the decay of M if it has a comparable or faster rate. To fully reveal these slow phases of M formation, we examined kinetics of M rise in the K96A mutant. In a separate study (to be published



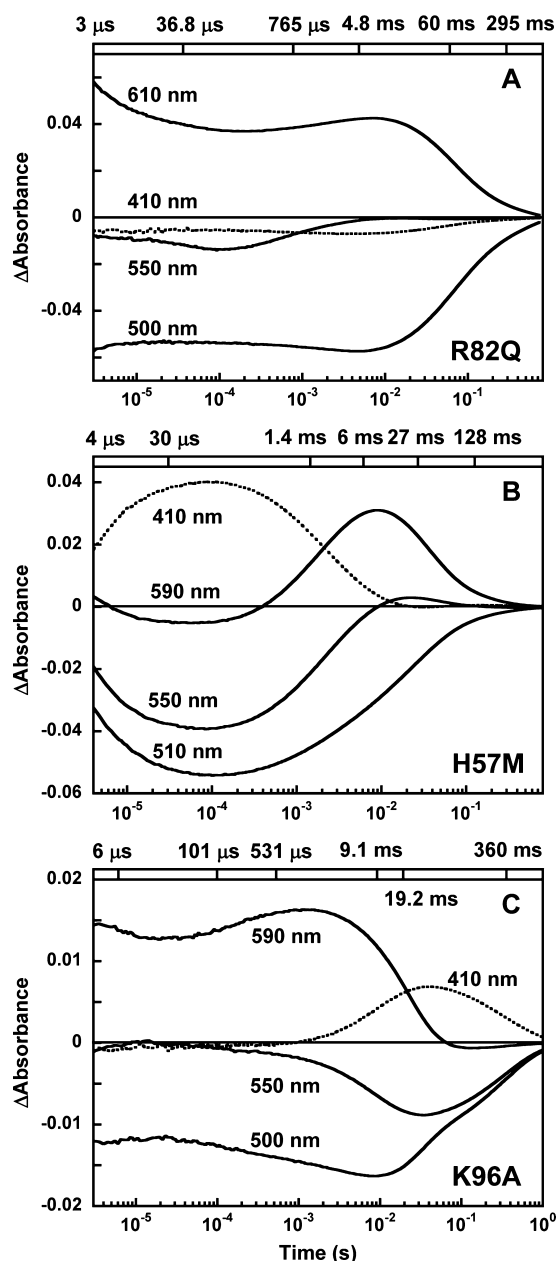


**Figure 7.** Kinetics of light-induced absorption changes in (A) the R82Q mutant at pH 9, (B) the H57M mutant at pH 7.6, and (C) the K96A mutant at pH 7.6.

elsewhere), we will show that substitution of Lys96 with alanine or glutamine dramatically slows the decay of M, like the D96N mutation in bacteriorhodopsin<sup>44</sup> and the E108Q mutation in proteorhodopsin.<sup>18</sup> The slower reprotonation of the Schiff base in the K96A mutant (360 ms at pH 7.6) allows us to observe formation of a slowly rising M with a time constant of ~12 ms (superposition of 9 and 19 ms components) (Figure 7C). Thus, we interpret the results for the K96A mutant as an indication that the M intermediate is formed at a pH well below the apparent  $pK_a$  of 9 for the accumulation of M in the wild type, but slowly. Accumulation of this slow component at neutral pH is apparently obscured in the wild type by the faster decay of the M intermediate (see Discussion).

**Kinetics of Light-Induced Proton Uptake and Release in the Photocycles of the Wild Type and the H57M Mutant.** The pH sensitive dye pyranine was used to follow the

kinetics of light-induced proton release and uptake at pH 7.2. An increase in pyranine absorbance corresponds to transient proton uptake by a protein from the bulk, while a decrease in absorbance corresponds to proton release. In the wild type, very little M accumulates at pH 7.2, but a substantial pyranine signal was observed (Figure 8). The time course reveals the

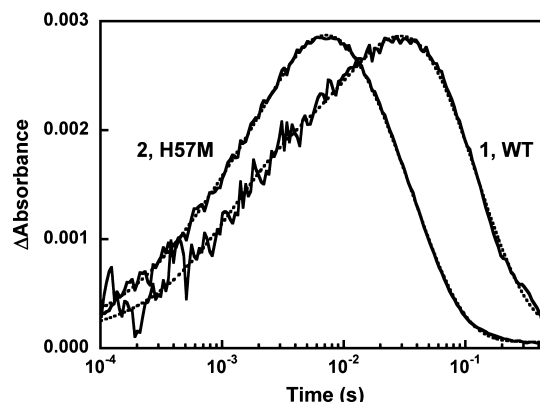


**Figure 8.** Kinetics of light-induced proton release and uptake after flash photoexcitation, followed by absorption changes of pyranine at 456 nm. Changes in the chromophore absorption were subtracted as explained in the text: (1) wild-type ESR at pH 7.2 and (2) H57M at pH 7.5. The measured wild-type ESR trace was multiplied by 3.6 to scale with that of H57M. Dashed lines are fits described in the text. Conditions: 0.2% DDM and 100 mM NaCl.

sequence of a proton uptake that was followed by a proton release, which is the same as in other eubacterial proton pumps at neutral pH<sup>13,14,18</sup> but the reverse of what is observed in bacteriorhodopsin.<sup>45</sup> In a control experiment, addition of 5 mM buffer (pH 7.2) reduced the magnitude of the pyranine signal by 85%. Proton uptake occurred with a time constant of ~12 ms [a better fit is obtained with a two-component rise, 1 ms (35%) and 16 ms (65%)], i.e., in good agreement with the kinetics of M decay and the rise of the red-shifted intermediate(s). This result supports the earlier conclusion reached with a pH sensitive dye (*p*-nitrophenol assayed at 400 nm<sup>3</sup>) that proton uptake occurs during the decay of M and the rise of the red-shifted intermediate. The release occurred with a ~120 ms time constant, which is somewhat slower than the decay of the absorbance at 590 nm.

Under similar conditions, both proton uptake and release were faster in the H57M mutant than in the wild type (Figure 8). Light-induced proton uptake occurred with a time constant of 1.8–2 ms, i.e., with very little delay or almost coincident with the decay of the M intermediate and the formation of the red-shifted photoproduct as in the wild type. Proton release occurred with a time constant of ~30 ms, coincident with the decay of the red-shifted intermediate (Figure 7B). These data indicate that the H57M mutation did not abolish proton uptake or release. A possible reason for the differences in the kinetics of the pyranine signal in the wild type and H57M is given in Discussion (see also Figure S5 of the Supporting Information).

**Chromophore Titration and Photocycle of ESR in Liposomes and a Lipid-like Detergent.** The specific  $pK_a$  values at which transitions take place in ESR were found to be sensitive to the environment, and this sensitivity seems to be stronger than in other retinal proteins. Despite this, incorporation into liposomes does not qualitatively affect the pH-induced behavior of ESR described above on the solubilized



sample. The main difference from the detergent-solubilized system is that the corresponding  $pK_a$  values are downshifted by 2–2.5 units. As seen for the solubilized samples, with an increase in pH the absorption maximum of wild-type ESR undergoes a 9 nm blue shift, from 540 to 531 nm, with a  $pK_a$  of  $\sim 6.5$  (Figure 9A), versus  $\sim 9$  in the solubilized samples (Figure 1B). The small magnitude of this blue shift implies partial protonation of Asp85 in the liposomes, as is the case in the solubilized samples. When full protonation of Asp85 can be expected, as in the H57M mutant (see above), the corresponding titration in liposomes reveals an at least 4-fold greater blue shift. Similar to the solubilized samples of H57M,

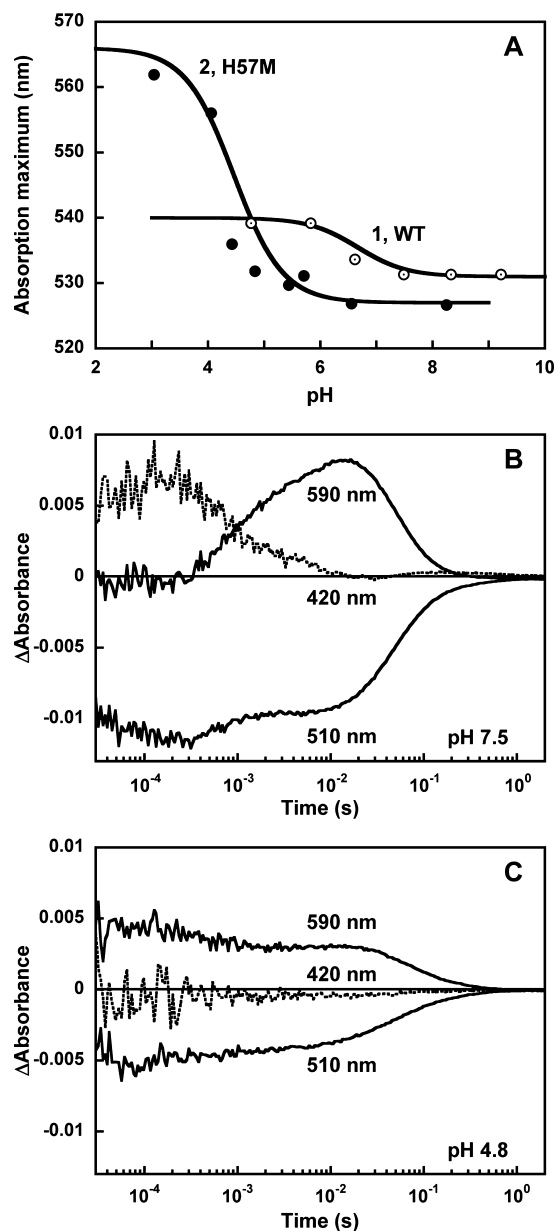


**Figure 9.** ESR incorporated into liposomes. (A) pH dependence of the absorption maximum in (1) the wild type, fit with a  $pK_a$  of  $\sim 6.5$ , and (2) the H57M mutant, fit with a  $pK_a$  of  $\sim 4.5$ . (B and C) Photocycle kinetics of wild-type ESR at selected wavelengths (420, 510, and 590 nm) at pH 7.5 (B) and 4.8 (C), i.e., above and below, respectively, the corresponding  $pK_a$  of  $\sim 6.5$  of the transition revealed by the shift in the absorption maximum.

where this shift is 45 nm, from 565 to 520 nm (Figure 2), in liposomes the corresponding blue shift is 39 nm, from 566 to 527 nm, and occurs with a  $pK_a$  of  $\sim 4.5$  (Figure 9A), versus a  $pK_a$  of 6.3 in detergent (Figure 6). Titration to pH  $< 4$  was not possible in liposomes because of aggregation problems. Strong scattering complicated also the fluorescence study of liposomes.

Qualitatively, the pattern of the photocycle in the liposomes is similar to that in detergent except that M decay is faster. Panels B and C of Figure 9 present time-resolved absorption traces after flash photoexcitation at pH values above and below the  $pK_a$  of  $\sim 6.5$ , respectively. As in detergent, the extent of accumulation of M increases with an increase in pH (Figure 9B) and its  $pK_a$  correlates with the  $pK_a$  of the transition revealed by the shift in the absorption maximum (Figure 9A). No M state accumulates at pH values below the  $pK_a$  of  $\sim 6.5$ . The data in Figure 9B characterize the photocycle of wild-type ESR in liposomes at pH  $\sim 7.5$  with large amounts of M present. In solubilized samples at this pH, almost no M is observed (Figure 5A), but because in liposomes this is approximately 1 pH unit above the  $pK_a$  of the spectral transition (with the 9 nm shift), the kinetics in Figure 9B should be compared instead to that at pH 10 in detergent (Figure 5C). The similarity between the kinetics in liposomes and in detergent above and below the corresponding  $pK_a$  values strongly indicates that in liposomes the observed  $pK_a$  values,  $\sim 6.5$  for the wild type and  $\sim 4.5$  for the H57M mutant (Figure 9A), correspond to the same molecular events that are observed with  $pK_a$  values of  $\sim 9$  for the wild type and 6.3 for the H57M mutant in detergent.

Accumulation of large amounts of the M intermediate and its fast rise in wild-type ESR at neutral pH in liposomes potentially provide an opportunity to correlate the kinetics of M with light-induced proton release and uptake under conditions of a presumably deprotonated His57. However, measurements of the pyranine signal in liposomes are complicated by light scattering, slow access of protons to the interior, and differences in pH inside and outside that develop during illumination. To overcome these problems, we screened detergents with the aim of finding one that would produce an environment for the protein similar to that in proteoliposomes. The one that comes close to mimicking lipids is 1-palmitoyl-2-hydroxy-*sn*-glycero-3-phospho(1'-*rac*-glycerol) sodium salt (16:0 Lyso PG, or LPG). LPG resembles a lipid (C16 hydrocarbon tail and a phosphate headgroup), but with only one of the OH groups of the glycerol esterified.<sup>46</sup> In this detergent, the protein is stable (although only at pH  $> 6$ ), the amount of M that accumulates increases with an apparent  $pK_a$  of 6.5 as in the liposomes, its rise is rapid as in the liposomes, and its decay is faster than in dodecyl maltoside (DDM) but similar to that in liposomes. The pyranine signal at pH 7.6 in 0.05% LPG showed the same pattern as in DDM: proton uptake that occurred during the decay of M, followed by a release at the end of the photocycle, both occurring faster than in DDM (see Figure S5 of the Supporting Information).

**pH Dependence of Proton Transport by ESR in *E. coli* Cells and in Liposomes.** Illumination of suspensions of *E. coli* cells with ESR expressed and reconstituted with all-*trans*-retinal caused large light-induced pH changes consistent with outwardly directed transport of protons (Figure 10A). The light-induced pH changes were abolished by 90% in 50  $\mu$ M CCCP and were absent in cells to which all-*trans*-retinal was not added. The pH changes were greatest between pH 5 and 6 and decreased substantially at pH  $< 4.5$  and  $> 8$ . The decreases might be caused not only by changes in the efficiency of the

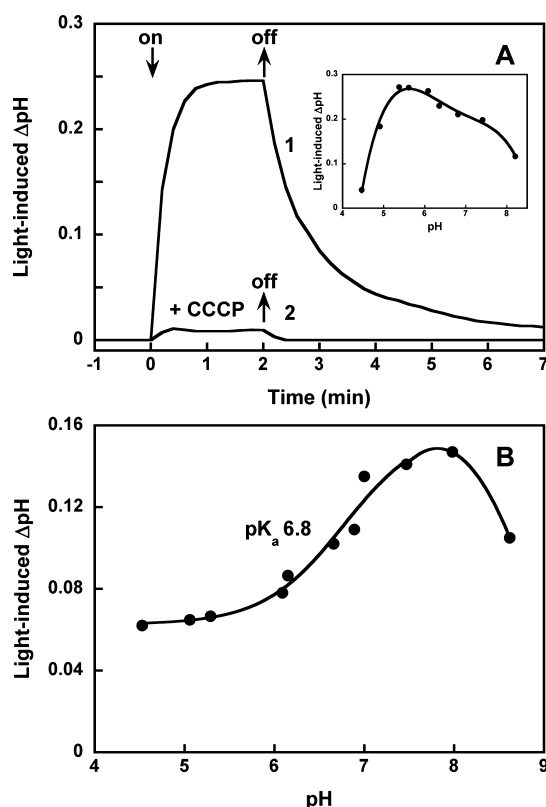


**Figure 10.** Light-induced outward proton pumping by ESR. (A) Time course of light-induced pH changes in a suspension of *E. coli* cells with ESR expressed and reconstituted with all-*trans*-retinal (1) and after addition of  $5 \times 10^{-5}$  M CCCP at pH 5.5 (2). The inset shows the pH dependence of light-induced pH changes in *E. coli* cells with ESR. (B) pH dependence of light-induced pH changes in a suspension of proteoliposomes containing ESR.

proton pump but also by a pH dependence in the internal buffering and the permeability of cell membrane to protons and other ions, as seen previously.<sup>47</sup> For example, at pH >7, the relaxation of the pH change after the light had been turned off was substantially faster than at pH 5. Large light-induced pH changes were observed also in liposomes reconstituted with ESR between pH 4.5 and 9, with a maximum at pH 8 (Figure 10B). The initial slope of light-induced acidification that presumably corresponds to the rate of the proton pump was, however, greatest between pH 4.5 and 6 and decreased at higher pH (not shown). Thus, both *E. coli* and liposomes with ESR exhibit large changes in pH from light-induced transport of protons between pH 4.5 and 8.5, indicating that ESR, when in a lipid environment, is a potent light-driven H<sup>+</sup> pump operating over a broad pH range.

## DISCUSSION

**Origin of the pH-Dependent Transitions in the Absorption Spectrum and Accumulation of the M Intermediate in Wild-Type ESR and Its Mutants.** In bacteriorhodopsin, the relationship of the absorption maximum of the chromophore, the protonation state of the proton acceptor (Asp85), and the deprotonation of the retinal Schiff base after photoexcitation is direct. Because of its interaction with the extracellular proton release group, Asp85 has two pK<sub>a</sub> values, but >99% deprotonates with the lower pK<sub>a</sub> of 2.6.<sup>48</sup> Above this pK<sub>a</sub>, Asp85 functions virtually fully as a proton

acceptor in the cycle.<sup>10</sup> This relationship does not hold for ESR, where accumulation of M does not coincide with the fraction of unprotonated Asp85 in the initial state.

There are several pK<sub>a</sub> values for the blue shifts in the spectral titration of the chromophore of wild-type ESR, as revealed most clearly when solubilized in detergent (DDM). As in bacteriorhodopsin, in ESR a major fraction of Asp85 is deprotonated with a pK<sub>a</sub> of ~2.3. However, unlike in the other protein, this transition does not correlate with accumulation of the M intermediate in the photocycle. The accumulation of M relates instead to a transition with a pK<sub>a</sub> of 9 in the solubilized protein and a pK<sub>a</sub> of 6.5 in liposomes, which corresponds to an only 10 nm blue shift in the absorption spectrum (Figure 1B), and we find that this is not from a transition in which Asp85 changes from a fully protonated to a fully deprotonated state, as in bacteriorhodopsin. This follows from the position of the absorption maximum in the wild type at pH 5 that is at a substantially shorter wavelength, at 534 nm, than in the H57M, at 565 nm, and D85N mutants, at 563 nm, suggesting that if the transition with a pK<sub>a</sub> of ~9 (Figure 1B) refers to deprotonation of Asp85 it can only be partial and involve a small fraction of the aspartate. Indeed, the chromophore fluorescence excitation spectra confirm that no more than 10% of Asp85 (Figure 3E) undergoes changes in protonation between pH 7 and 10.

We suggest that both the absorption shift and increase in yield of M at high pH are controlled by the deprotonation of another residue that closely interacts with Asp85. It cannot be Arg82 but is probably His57. The evidence of such involvement of His57 comes from the properties of the H57M mutant. (i) The overall pH-induced blue shift of the absorption maximum is 4–5 times larger than in the wild type (Figures 2B and 9A). (ii) It occurs mainly with a single pK<sub>a</sub> that is 2–2.5 pH units lower than in the wild type. (iii) The fluorescence excitation spectra of H57M indicate that its large spectral shift with a pK<sub>a</sub> of 6.3 (from 565 to 518 nm) originates from full deprotonation of Asp85. (iv) The absorption shift with a pK<sub>a</sub> of 9 seen in the wild type, which is caused by deprotonation of a group affecting the proton affinity of Asp85, is apparently absent in the mutant. Thus, substitution of His57 with methionine or asparagine converts ESR to a pigment that, except for a higher pK<sub>a</sub> of the proton acceptor Asp85, appears to behave quite similarly to bacteriorhodopsin with respect to the relationship between the yield of M and the protonation state of the counterion. No change in the accumulation of M is observed in H57M in DDM between pH 8 and 10, consistent with the suggestion above that it is deprotonation of His57 that is responsible for changes in the kinetics and yield of M at pH ~9.

Deprotonation of His57 above pH 9 (or pH 6.5 in liposomes) might cause a blue shift and affect M formation in three possible ways. The first is electrostatic but without specificity: removal of any positive charge near Asp85 should facilitate a transfer of the proton to it from the Schiff base. However, replacement of the other positively charged residue near Asp85, i.e., Arg82, does not have such an effect. A second possible mechanism holds that when His57 is protonated, the retinal is not all-*trans* but 13-*cis*,15-*syn*, as in dark-adapted bacteriorhodopsin where this isomeric state produces little or no M.<sup>49</sup> In this alternative, deprotonation of His57 would convert the pigment to the all-*trans* form. This seems unlikely in view of the fact that there are few retinal proteins or mutants in which the 13-*cis*,15-*syn* form is the exclusive isomeric form, and in any case, conversion to the all-*trans* form is expected to

cause a red shift in the maximum, not a blue shift. The third alternative is that the interaction of Asp85 with protonated His57 removes a sufficient fraction of the negative charge of the anionic aspartate to abolish, or slow, the transfer of a proton to it from the Schiff base. In this case, elimination of the salt bridge between His57 and Asp85, either at pH 9 or by removal of His57 in mutants, will move negative charge back to Asp85, which would both cause a blue shift and restore M formation. This hypothetical scenario needs further verification by means of crystallography and NMR, as the latter would yield the  $pK_a$  of His57 in this protein. With respect to the former, it is worth mentioning that in xanthorhodopsin, to date the only eubacterial pump with a known structure, the distance between the carboxyl group of Asp and the His nitrogen is quite short, 2.5 Å, suggesting a strong hydrogen bond. The conformation of the carboxyl group is different from that of Asp85 in BR, which lacks a His.<sup>13</sup> With respect to the latter, the  $pK_a$  of the homologous His in proteorhodopsin was determined to be 6–8 (see below), after reconstitution into liposomes, via solid state NMR.<sup>21</sup>

It appears further that in the absence of His the principal  $pK_a$  of Asp85 is ~4 units higher than in its presence, which is ~2.3 (Figure 1B). Evidently, His57 in the wild type keeps the Asp85 mostly deprotonated even at very low pH. Deprotonation of His57 at pH >8 would presumably result in an increase in the proton affinity of Asp85 ( $pK_a$ ) and facilitation of M formation. The evidence of the coupling of the  $pK_a$  values of the two residues, besides the properties of the H57M and H57N mutants, is the complex pH dependence of the fraction of protonated Asp85 in wild-type ESR, which exhibits a second decrease with a  $pK_a$  of 9 (Figure 3E). Such complex titration is a sign of coupling, and the  $pK_a$  of 9 corresponds to the deprotonation of a residue that affects the  $pK_a$  of Asp85. In bacteriorhodopsin, such a group is a proton release complex,<sup>43,48</sup> whereas in ESR, it appears to be His57. Interestingly, there is a precedent among bacteriorhodopsin mutants for which Asp85 is unprotonated but M is not formed. It is the R82H mutant for which the  $pK_a$  of Asp85 is decreased to 1, whereas M formation is observed only at pH >3.<sup>50</sup>

**Function of His57 in ESR. Comparison of ESR with Other Retinal Proton Pumps.** ESR, xanthorhodopsin, and *Gloeobacter* rhodopsin share several features with proteorhodopsin (presence of His and lack of a specialized proton release group analogous to the Glu194-Glu204 pair in bacteriorhodopsin), and they exhibit a broader pH range of functionality (lower  $pK_a$  of the counterion). A complex titration of the counterion seen in ESR that potentially allows a significant fraction of the protein to function at low pH is likely to be their common feature. The measurements of light-induced changes in suspensions of cells and liposomes show that wild-type ESR can pump protons at a pH as low as 4.5, i.e., at a lower pH than would be predicted from the  $pK_a$  of 6.5 for accumulation of M in the liposomes (Figure 9A). It appears that the role of His57 in ESR is to keep Asp85 unprotonated at physiological pH, down to at least pH 4, so that it can function as a proton acceptor in this pH range. The pH of the samples of permafrost where *E. sibiricum* was collected was near neutral, pH 7.3.<sup>1</sup> The pH and ionic strength being lower than in the marine environment characteristic for proteorhodopsin correlates with the ability of ESR to pump protons at a pH as low as 4.5.

Removal of His57 does not eliminate the ability to transport protons as was also observed for the analogous proteorhodopsin mutants.<sup>12,21</sup>

Several observations with ESR that suggest complex titration of its counterion are similar to those we had made with xanthorhodopsin where only a small 3–5 nm shift in the absorption maximum was detected between pH 4 and 10<sup>20</sup> that was accompanied by an only 2.5-fold increase in the chromophore fluorescence intensity.<sup>26</sup> In the related *Gloeobacter* rhodopsin, a large, 23 nm, difference between the chromophore absorption spectrum and the fluorescence excitation spectrum indicated the presence of a minor fraction of the pigment with a protonated counterion,<sup>51</sup> as in ESR. These features can be explained assuming a strong Asp–His hydrogen bond, as revealed by the crystal structure of xanthorhodopsin.<sup>13</sup>

Studies of the green-absorbing proteorhodopsin produced two models for His–Asp interaction. Bergo et al.<sup>12</sup> suggested, from FTIR spectra and mutagenesis, that His75 interacts with Asp97, the residues homologous to His57 and Asp85 in ESR, respectively. His75 is protonated over a wide pH range, up to pH 9, but is deprotonated during the photocycle when the salt bridge between the two residues is suggested to be broken upon protonation of Asp97 during M formation. A different picture was drawn from solid state NMR<sup>21</sup> with respect to the protonation state of His75, which according to this study is protonated only up to pH 6 and is deprotonated in the initial state between pH 6 and 8, over a pH range where Asp97 also is deprotonated. Both studies suggest, from titration of the spectral shifts of the chromophore, that the  $pK_a$  of Asp97 is 7.5 (compared to the much lower value, 2.6, for the homologous aspartate residue in bacteriorhodopsin) and that hydrogen bonding to His75 is responsible for the high  $pK_a$ . However, this difference in the  $pK_a$  could not be attributed solely or even mainly to the His because the H75M mutation decreased the  $pK_a$  by only 0.8 unit (a somewhat larger decrease, from 7.5 to 5.3, was produced by the H75N mutation).<sup>21</sup> According to the NMR spectra, the proton in His is localized on NE2 (as in free solution), so that ND1 stabilizes the protonated state of the Asp at pH >6.<sup>21</sup>

It should be noted that interpretation of results with proteorhodopsin in terms of a single  $pK_a$  did not take into account the smaller than expected blue shifts that could indicate the possibility of partial titration, in analogy to ESR solubilized in detergent. Complex titration of the counterion might occur also in proteorhodopsin because the fluorescence spectra at pH 6 and 9 were found to be similar in amplitude and the excitation spectrum showed a maximum at 565 nm,<sup>52</sup> which is red-shifted from the absorption maximum at 521 nm at both pH values. This might indicate the presence of a species with protonated Asp97 in substantial amounts even at pH 9.

The order of proton release and uptake in the eubacterial rhodopsins is an interesting question, as it bears on the mechanism of proton release machinery in the eubacterial rhodopsins that is different from that in bacteriorhodopsin. Two kinds of light-induced pH changes were observed in proteorhodopsin. In measurements with pyranine on *E. coli* membranes containing proteorhodopsin at pH 7.9, proton uptake occurred first, during the rise of the red-shifted photoproduct (N) formed from M. It was followed by proton release at the end of the photocycle during the decay of the red-shifted intermediate(s).<sup>18</sup> This sequence indicated the absence of a specialized proton release group similar to that of bacteriorhodopsin and suggested that the released proton might originate from deprotonation of Asp97 (homologous to Asp85 in bacteriorhodopsin) at the end of the photocycle. A



similar sequence of uptake followed by release was reported for *Gloeobacter* rhodopsin,<sup>14</sup> for xanthorhodopsin,<sup>13</sup> and here for ESR. On the other hand, measurements by Krebs et al.<sup>53</sup> at pH 9.5 in diheptanoylphosphatidylcholine micelles resulted in a proton signal with a reversed polarity: proton release first (20  $\mu$ s), followed by proton uptake (0.3 s) somewhat earlier than the decay of the slow component of M and completion of the photocycle (0.6 s).<sup>53</sup> A subsequent FTIR study suggested that the release cannot be from Asp97 because it remained protonated in this time domain.<sup>54</sup> A study of the pH dependence of proton release and uptake with a pH sensitive  $\text{SnO}_2$  electrode by Tamogami et al. confirmed these two different kinds of signals,<sup>55</sup> at neutral and high pH. They observed both patterns in lipid-reconstituted proteorhodopsin and found that the switch between the two is determined by the pH. The reason for the variability of the order of transient release and uptake is unknown, but it is clear that it is not the presence or absence of lipid. Generally, light-induced pH changes might originate not only from transmembrane proton transport but also from transient protonation and deprotonation of residues experiencing changes in  $pK_a$  during the photocycle. Further studies of ESR at different pH values and mutants of ESR (in progress) should clarify whether both types of light-induced pH changes take place in this protein also and shed light on their origin.

**Possible Reasons for the Absence of Accumulation of the M State at pH <8 in Wild-Type ESR Solubilized in Detergent.** Little or no M accumulates in the wild-type photocycle at pH <8 (Figure 6) where Asp85 is mostly deprotonated and presumably His57 is protonated. Such a situation can arise when the rise of M is much slower than its decay. The evidence that this is the case comes from experiments with the K96A and H57M mutants and transport by ESR in liposomes. Reprotonation of the Schiff base (the decay of M) is slowed by the K96A mutation by more than 10-fold, and under these conditions, accumulation of the M intermediate in DDM becomes clearly visible at a pH as low as 7.6 (Figure 7C); in the wild type, it was barely detectable at this pH (Figure 5A). The rise of this slowly accumulating M in K96A is  $\sim 12$  ms (it is biphasic with a major and a minor component, with time constants of 9 and 19 ms, respectively). In the wild type, the slow component of M rise at pH 7.6 is  $\sim 4.8$  ms whereas the M decay is 50 ms. Conversely, in H57M, where the rise of M is very rapid, the decay of M is seen to occur with a 1.4 ms lifetime at the same pH. The greatly diminished level of accumulation of M in the wild-type photocycle at neutral pH can be explained if one assumes that M formation occurs much slower than at pH 9, so that the actual time constants for M formation and decay are close to those in the K96A and H57M mutants, respectively, i.e., the reverse of the apparent, i.e., observed, ones. This would result in a decrease of the amplitude of M by more than 1 order of magnitude and explain the apparent lack of accumulation of M at neutral pH. This model can also explain features of the pyranine signal of ESR in DDM, its reduced amplitude, and a slower rise, which tracks accumulation of the red-shifted species (that reflects the slow M rise). A well-known example of a situation with reversed apparent time constants of rise and decay is the O intermediate of bacteriorhodopsin, whose decay is faster than its formation.<sup>56–59</sup> An unlikely alternative explanation for the lack of accumulation of M in ESR in detergent at pH  $\leq 7.6$  would be a mode of pumping without M formation (i.e., transient deprotonation of the Schiff base)

when a proton is supplied to Asp85 from His after the retinal photoisomerization and subsequently replenished from the cytoplasmic side via Lys96. This would be unprecedented. An example of a system that transports protons without apparent M accumulation is the R82Q/D212N double mutant of bacteriorhodopsin, but the lack of M occurs for kinetic reasons.<sup>60</sup>

How would the protonation state of His57 affect the transfer of a proton from the Schiff base to Asp85? It is possible that to form the M state, the Asp–His interaction must be broken as suggested for PR,<sup>12</sup> and it occurs slowly when His57 is protonated so that M does not accumulate. When His57 is mostly deprotonated in the initial state, at pH >9, M formation becomes very fast. A similar phenomenon is observed in the photocycle of bacteriorhodopsin when deprotonation of the proton release group associated with that change in the conformation of Arg82 results in a dramatic acceleration of M formation.<sup>29</sup>

An interesting difference between ESR and bacteriorhodopsin is that in ESR neutralization of Arg82 did not cause substantial changes in the pH dependence of the absorption spectrum and suppressed accumulation of M at high pH values, whereas in BR, the R82Q or R82A mutation increases the  $pK_a$  of Asp85 by  $\sim 4.8$  units and facilitates faster M formation.<sup>31,61</sup> This most probably reflects a different function and hydrogen bonding pattern of Arg82, like that in xanthorhodopsin, in which the distance from the Arg82 homologue's side chain to the homologue of Asp85 is larger than in bacteriorhodopsin.<sup>13</sup> This implies that the crystallographic structure of XR represents features common to other eubacterial proton pumps. This might be especially true for ESR and *Gloeobacter* rhodopsin, which are similar to XR in that they do not exhibit large absorption shifts between pH 5 and 9.<sup>14,26,51</sup>

**Comparison of ESR in Solubilized DDM and in Proteoliposomes.** The optical properties of proteoliposomes precluded pH dependence studies with the same details as we present above for detergent-solubilized ESR. However, all our data indicate that the two systems, lipid versus detergent, produce, when corrected for the shift of the  $pK_a$  values of the major changes in the Asp–His complex, the same pH-dependent patterns of the photocycle and the shifts in the absorption maximum in all the mutants studied so far. Detergent-dependent changes as large as those for the  $pK_a$  of the high-pH transition, from pH 9 (in DDM) to pH 6.5 (in liposomes), are unprecedented. In proteorhodopsin, for example, this difference is only  $\sim 0.6$  pH unit (the  $pK_a$  value at which the major changes in the Asp–His complex occur is within the range of 7.1–7.7 in the pigment in liposomes, solubilized in DDM, in *E. coli* cells, and in membranes).<sup>18,62–64</sup>

## CONCLUSIONS

In DDM-solubilized ESR, between pH 3 and 10, the pH dependence of the ESR chromophore absorption band is complex but the major fraction of the Schiff base counterion, Asp85, is unprotonated. Substitution of His57 with methionine or asparagine causes the counterion to undergo complete protonation with a single  $pK_a$  of 6.3. This indicates strong interaction between Asp85 and His57 that preserves the unprotonated state of the counterion even at low pH. In the H57M and H57N mutants, the yield of the M intermediate coincides with the fraction of protein with a deprotonated counterion ( $pK_a$  value of 6.3 in DDM or 4.5 in liposomes). In the wild type, this is not so: the dramatic increase in the



fraction of M formed (with a  $pK_a$  of  $\sim 9$  in DDM or  $\sim 6.5$  in LPG and liposomes) correlates with a small,  $\sim 10$  nm, blue shift of the absorption maximum with a similar  $pK_a$  that is apparently unrelated to the change in the protonation state of the major fraction of Asp85. Fluorescence measurements confirm that this transition is not primarily from deprotonation of the counterion. The  $pK_a$  of 9 refers to deprotonation of only a small fraction of the Asp85 ( $\leq 10\%$ ), and this transition is caused by deprotonation of another residue. It is not the Arg82, and we presume that it is His57, that affects the  $pK_a$  of Asp85 and the rate of its protonation by the retinal Schiff base in the photocycle.

## ■ ASSOCIATED CONTENT

### ■ Supporting Information

Scans of sodium dodecyl sulfate–acrylamide gels showing removal of a six-His tag of ESR by thrombin (Figure S1), a comparison of the light-induced absorption changes in wild-type ESR with a six-His tag (A and B) and with the six-His tag cleaved (Figure S2), the pH dependence of the fluorescence spectra and fluorescence intensity of the chromophore of the H57M mutant of ESR (Figure S3), the kinetics of absorption changes at selected wavelengths in the H57R mutant induced by laser flashes (Figure S4), and the kinetics of light-induced absorption changes of the pH sensitive dye pyranine at 455 nm and the kinetics of absorption changes at 410 nm in ESR solubilized in 0.05% 16:0 Lyso-PG (Figure S5). This material is available free of charge via the Internet at <http://pubs.acs.org>.

## ■ AUTHOR INFORMATION

### Corresponding Authors

\*S.P.B.: Department of Physiology and Biophysics, C-335 Medical Sciences I, University of California, Irvine, CA 92697-4560; e-mail, [balashov@uci.edu](mailto:balashov@uci.edu); phone, (949) 824-2720.

\*J.K.L.: Department of Physiology and Biophysics, D320 Medical Sciences I, University of California, Irvine, CA 92697-4560; e-mail, [jklanyi@uci.edu](mailto:jklanyi@uci.edu); phone, (949) 824-7150; fax, (949) 824-8540.

\*L.E.P.: Shemyakin and Ovchinnikov Institute of Bioorganic Chemistry, ul. Miklukho-Maklaya, 16/10, 117997 Moscow, GSP-7, Russian Federation; e-mail, [lpetr65@yahoo.com](mailto:lpetr65@yahoo.com); phone, +7 (495) 330 6983; fax, +7 (495) 330-6983.

### Funding

We acknowledge support from the National Institutes of Health (GM29498 to J.K.L.) to fund time-resolved spectral measurements; the Division of Chemical Sciences, Geosciences, and Biosciences, Office of Basic Energy Sciences of the U.S. Department of Energy (DEFG03-86ER13525 to J.K.L.), to fund laser kinetic spectroscopy; ARO (W911NF-09-1-0243 to S.P.B.) to fund fluorescence spectroscopy; the Federal Targeted Program on Scientific and Scientific-Pedagogical Staff of Innovative Russia (to L.E.P.); and the Molecular and Cell Biology Program of the Russian Academy of Science (to D.A.D.) to fund creation and purification of mutants.

### Notes

The authors declare no competing financial interest.

## ■ ACKNOWLEDGMENTS

We thank E. A. Kryukova for expert technical assistance.

## ■ ABBREVIATIONS

DDM, *n*-dodecyl  $\beta$ -D-maltopyranoside; MES, 2-(*N*-morpholino)ethanesulfonic acid; MOPS, 3-(*N*-morpholino)propanesulfonic acid; HEPES, 4-(2-hydroxyethyl)-1-piperazineethanesulfonic acid; CHES, *N*-cyclohexyl-2-aminoethanesulfonic acid; CAPS, *N*-cyclohexyl-3-aminopropanesulfonic acid; CCCP, carbonyl cyanide *m*-chlorophenylhydrazone; LPG, 1-palmitoyl-2-hydroxy-*sn*-glycero-3-phospho(1'-*rac*-glycerol); BR, bacteriorhodopsin.

## ■ REFERENCES

- (1) Vishnivetskaya, T., Kathariou, S., McGrath, J., Gilichinsky, D., and Tiedje, J. M. (2000) Low-temperature recovery strategies for the isolation of bacteria from ancient permafrost sediments. *Extremophiles* 4, 165–173.
- (2) Rodrigues, D. F., Goris, J., Vishnivetskaya, T., Gilichinsky, D., Thomashow, M. F., and Tiedje, J. M. (2006) Characterization of *Exiguobacterium* isolates from the Siberian permafrost. Description of *Exiguobacterium sibiricum* sp. nov. *Extremophiles* 10, 285–294.
- (3) Petrovskaya, L. E., Lukashev, E. P., Chupin, V. V., Sychev, S. V., Lyukmanova, E. N., Kryukova, E. A., Ziganshin, R. H., Spirina, E. V., Rivkina, E. M., Khatypov, R. A., Erokhina, L. G., Gilichinsky, D. A., Shuvalov, V. A., and Kirpichnikov, M. P. (2010) Predicted bacteriorhodopsin from *Exiguobacterium sibiricum* is a functional proton pump. *FEBS Lett.* 584, 4193–4196.
- (4) Oesterhelt, D., and Stoekenius, W. (1973) Functions of a new photoreceptor membrane. *Proc. Natl. Acad. Sci. U.S.A.* 70, 2853–2857.
- (5) Ovchinnikov, Y. A., Abdulaev, N. G., Feigina, M. Y., Kiselev, A. V., and Lobanov, N. A. (1979) The structural basis of the functioning of bacteriorhodopsin: An overview. *FEBS Lett.* 100, 219–224.
- (6) Khorana, H. G., Gerber, G. E., Herlihy, W. C., Gray, C. P., Anderregg, R. J., Nihei, K., and Biemann, K. (1979) Amino acid sequence of bacteriorhodopsin. *Proc. Natl. Acad. Sci. U.S.A.* 76, 5046–5050.
- (7) Bèjà, O., Aravind, L., Koonin, E. V., Suzuki, M. T., Hadd, A., Nguyen, L. P., Jovanovich, S. B., Gates, C. M., Feldman, R. A., Spudich, J. L., Spudich, E. N., and DeLong, E. F. (2000) Bacterial rhodopsin: Evidence for a new type of phototrophy in the sea. *Science* 289, 1902–1906.
- (8) Balashov, S. P., Imasheva, E. S., Boichenko, V. A., Antón, J., Wang, J. M., and Lanyi, J. K. (2005) Xanthorhodopsin: A proton pump with a light-harvesting carotenoid antenna. *Science* 309, 2061–2064.
- (9) Mongodin, E. F., Nelson, K. E., Daugherty, S., DeBoy, R. T., Wister, J., Khouri, H., Weidman, J., Walsh, D. A., Papke, R. T., Sanchez Perez, G., Sharma, A. K., Nesbø, C. L., MacLeod, D., Baptiste, E., Doolittle, W. F., Charlebois, R. L., Legault, B., and Rodriguez-Valera, F. (2005) The genome of *Salinibacter ruber*: Convergence and gene exchange among hyperhalophilic bacteria and archaea. *Proc. Natl. Acad. Sci. U.S.A.* 102, 18147–18152.
- (10) Subramaniam, S., Greenhalgh, D. A., and Khorana, H. G. (1992) Aspartic acid 85 in bacteriorhodopsin functions both as proton acceptor and negative counterion to the Schiff base. *J. Biol. Chem.* 267, 25730–25733.
- (11) Rangarajan, R., Galan, J. F., Whited, G., and Birge, R. R. (2007) Mechanism of spectral tuning in green-absorbing proteorhodopsin. *Biochemistry* 46, 12679–12686.
- (12) Berge, V. B., Sineshchikov, O. A., Kralj, J. M., Partha, R., Spudich, E. N., Rothschild, K. J., and Spudich, J. L. (2009) His-75 in proteorhodopsin, a novel component in light-driven proton translocation by primary pumps. *J. Biol. Chem.* 284, 2836–2843.
- (13) Luecke, H., Schobert, B., Stagno, J., Imasheva, E. S., Wang, J. M., Balashov, S. P., and Lanyi, J. K. (2008) Crystallographic structure of xanthorhodopsin, the light-driven proton pump with a dual chromophore. *Proc. Natl. Acad. Sci. U.S.A.* 105, 16561–16565.
- (14) Miranda, M. R. M., Choi, A. R., Shi, L., Bezerra, A. G., Jung, K.-H., and Brown, L. S. (2009) The photocycle and proton translocation

pathway in a cyanobacterial ion-pumping rhodopsin. *Biophys. J.* 96, 1471–1481.

(15) Braiman, M. S., Mogi, T., Marti, M., Stern, L. J., Khorana, H. G., and Rothschild, K. J. (1988) Vibrational spectroscopy of bacteriorhodopsin mutants: Light-driven proton transport involves protonation changes of aspartic acid residues 85, 96, and 212. *Biochemistry* 27, 8516–8520.

(16) Gerwert, K., Hess, B., Soppa, J., and Oesterhelt, D. (1989) Role of aspartate-96 in proton translocation by bacteriorhodopsin. *Proc. Natl. Acad. Sci. U.S.A.* 86, 4943–4947.

(17) Miller, A., and Oesterhelt, D. (1990) Kinetic optimization of bacteriorhodopsin by aspartic acid 96 as an internal proton donor. *Biochim. Biophys. Acta* 1020, 57–64.

(18) Dioumaev, A. K., Brown, L. S., Shih, J., Spudich, E. N., Spudich, J. L., and Lanyi, J. K. (2002) Proton transfers in the photochemical reaction cycle of proteorhodopsin. *Biochemistry* 41, 5348–5358.

(19) Friedrich, T., Geibel, S., Kalmbach, R., Chizhov, I., Ataka, K., Heberle, J., Engelhard, M., and Bamberg, E. (2002) Proteorhodopsin is a light-driven proton pump with variable vectoriality. *J. Mol. Biol.* 321, 821–838.

(20) Imasheva, E. S., Balashov, S. P., Wang, J. M., and Lanyi, J. K. (2006) pH-dependent transitions in xanthorhodopsin. *Photochem. Photobiol.* 82, 1406–1413.

(21) Hempelmann, F., Holper, S., Verhoeven, M. K., Woerner, A. C., Kohler, T., Fiedler, S. A., Pfeiffer, N., Wachtveitl, J., and Glaubit, C. (2011) His75-Asp97 Cluster in Green Proteorhodopsin. *J. Am. Chem. Soc.* 133, 4645–4654.

(22) Horton, R. M., Hunt, H. D., Ho, S. N., Pullen, J. K., and Pease, L. R. (1989) Engineering hybrid genes without the use of restriction enzymes: Gene-splicing by overlap extension. *Gene* 77, 61–68.

(23) Bayley, H., Hojberg, B., Huang, K.-S., Khorana, H. G., Liao, M.-J., Lind, C., and London, E. (1982) Delipidation, renaturation, and reconstitution of bacteriorhodopsin. *Methods Enzymol.* 88, 74–81.

(24) Gidden, J., Denson, J., Liyanage, R., Ivey, D. M., and Lay, J. O. (2009) Lipid compositions in *Escherichia coli* and *Bacillus subtilis* during growth as determined by MALDI-TOF and TOF/TOF mass spectrometry. *Int. J. Mass Spectrom.* 283, 178–184.

(25) Martinez, A., Bradley, A. S., Waldbauer, J. R., Summons, R. E., and DeLong, E. F. (2007) Proteorhodopsin photosystem gene expression enables photophosphorylation in a heterologous host. *Proc. Natl. Acad. Sci. U.S.A.* 104, 5590–5595.

(26) Balashov, S. P., Imasheva, E. S., Wang, J. M., and Lanyi, J. K. (2008) Excitation energy-transfer and the relative orientation of retinal and carotenoid in xanthorhodopsin. *Biophys. J.* 95, 2402–2414.

(27) Govindjee, R., Balashov, S. P., and Ebrey, T. G. (1990) Quantum efficiency of the photochemical cycle of bacteriorhodopsin. *Biophys. J.* 58, 597–608.

(28) Dioumaev, A. K. (1997) Evaluation of intrinsic chemical kinetics and transient product spectra from time-resolved spectroscopic data. *Biophys. Chem.* 67, 1–25.

(29) Balashov, S. P., Imasheva, E. S., Ebrey, T. G., Chen, N., Menick, D. R., and Crouch, R. K. (1997) Glutamate-194 to cysteine mutation inhibits fast light-induced proton release in bacteriorhodopsin. *Biochemistry* 36, 8671–8676.

(30) Subramaniam, S., Marti, T., and Khorana, H. G. (1990) Protonation state of Asp (Glu)-85 regulates the purple-to-blue transition in bacteriorhodopsin mutants Arg-82 → Ala and Asp-85 → Glu: The blue form is inactive in proton translocation. *Proc. Natl. Acad. Sci. U.S.A.* 87, 1013–1017.

(31) Balashov, S. P., Govindjee, R., Kono, M., Imasheva, E., Lukashov, E., Ebrey, T. G., Crouch, R. K., Menick, D. R., and Feng, Y. (1993) Effect of the arginine-82 to alanine mutation in bacteriorhodopsin on dark adaptation, proton release, and the photochemical cycle. *Biochemistry* 32, 10331–10343.

(32) Luecke, H., Schobert, B., Richter, H.-T., Cartailler, J.-P., and Lanyi, J. K. (1999) Structure of bacteriorhodopsin at 1.55 Å resolution. *J. Mol. Biol.* 291, 899–911.

(33) Partha, R., Krebs, R., Caterino, T. L., and Braiman, M. S. (2005) Weakened coupling of conserved arginine to the proteorhodopsin

chromophore and its counterion implies structural differences from bacteriorhodopsin. *Biochim. Biophys. Acta* 1708, 6–12.

(34) Fischer, U., and Oesterhelt, D. (1979) Chromophore equilibria in bacteriorhodopsin. *Biophys. J.* 28, 211–230.

(35) Mowery, P. C., Lozier, R. H., Chae, Q., Tseng, Y.-W., Taylor, M., and Stoekenius, W. (1979) Effect of acid pH on the absorption spectra and photoreactions of bacteriorhodopsin. *Biochemistry* 18, 4100–4107.

(36) Kouyama, T., Kinoshita, K., and Ikegami, A. (1985) Excited-state dynamics of bacteriorhodopsin. *Biophys. J.* 47, 43–54.

(37) Balashov, S. P., Litvin, F. F., and Sineshchikov, V. A. (1988) Photochemical processes of light energy transformation in bacteriorhodopsin. In *Physicochemical Biology Reviews* (Skulachev, V. P., Ed.) pp 1–61, Harwood Academic Publishers GmbH, Basingstoke, U.K.

(38) Song, L., El-Sayed, M. A., and Lanyi, J. K. (1993) Protein catalysis of the retinal subpicosecond photoisomerization in the primary process of bacterial photosynthesis. *Science* 261, 891–894.

(39) Huber, R., Kohler, T., Lenz, M. O., Bamberg, E., Kalmbach, R., Engelhard, M., and Wachtveitl, J. (2005) pH-dependent photoisomerization of retinal in proteorhodopsin. *Biochemistry* 44, 1800–1806.

(40) Lenz, M. O., Woerner, A. C., Glaubit, C., and Wachtveitl, J. (2007) Photoisomerization in proteorhodopsin mutant D97N. *Photochem. Photobiol.* 83, 226–231.

(41) Lozier, R. H., Bogomolni, R. A., and Stoekenius, W. (1975) Bacteriorhodopsin: A light-driven proton pump in *Halobacterium halobium*. *Biophys. J.* 15, 955–963.

(42) Liu, S. Y. (1990) Light-induced currents from oriented purple membrane. I. Correlation of the microsecond component (B2) with the L-M photocycle transition. *Biophys. J.* 57, 943–950.

(43) Balashov, S. P. (2000) Protonation reactions and their coupling in bacteriorhodopsin. *Biochim. Biophys. Acta* 1460, 75–94.

(44) Otto, H., Marti, T., Holtz, M., Mogi, T., Lindau, M., Khorana, H. G., and Heyn, M. P. (1989) Aspartic acid-96 is the internal proton donor in the reprotonation of the Schiff base of bacteriorhodopsin. *Proc. Natl. Acad. Sci. U.S.A.* 86, 9228–9232.

(45) Zimányi, L., Váró, G., Chang, M., Ni, B., Needleman, R., and Lanyi, J. K. (1992) Pathways of proton release in the bacteriorhodopsin photocycle. *Biochemistry* 31, 8535–8543.

(46) Stafford, R. E., Fanni, T., and Dennis, E. A. (1989) Interfacial properties and critical micelle concentration of lysophospholipids. *Biochemistry* 28, 5113–5120.

(47) Ramos, S., Schuldiner, S., and Kaback, H. R. (1976) Electrochemical gradient of protons and its relationship to active transport in *Escherichia coli* membrane-vesicles. *Proc. Natl. Acad. Sci. U.S.A.* 73, 1892–1896.

(48) Balashov, S. P., Imasheva, E. S., Govindjee, R., and Ebrey, T. G. (1996) Titration of aspartate-85 in bacteriorhodopsin: What it says about chromophore isomerization and proton release. *Biophys. J.* 70, 473–481.

(49) Lozier, R. H., Niederberger, W., Ottolenghi, M., Sivorinovskiy, G., and Stoekenius, W. (1978) On the photocycles of light- and dark-adapted bacteriorhodopsin. In *Energetics and Structure of Halophilic Microorganisms* (Caplan, S. R., and Ginzburg, M., Eds.) Elsevier/North-Holland Biomedical Press, Amsterdam.

(50) Imasheva, E. S., Balashov, S. P., Ebrey, T. G., Chen, N., Crouch, R. K., and Menick, D. R. (1999) Two groups control light-induced Schiff base deprotonation and the proton affinity of Asp<sup>85</sup> in the Arg<sup>82</sup>His mutant of bacteriorhodopsin. *Biophys. J.* 77, 2750–2763.

(51) Imasheva, E. S., Balashov, S. P., Choi, A. R., Jung, K.-H., and Lanyi, J. K. (2009) Reconstitution of *Gloeobacter violaceus* rhodopsin with a light-harvesting carotenoid antenna. *Biochemistry* 48, 10948–10955.

(52) Lenz, M. O., Huber, R., Schmidt, B., Gilch, P., Kalmbach, R., Engelhard, M., and Wachtveitl, J. (2006) First steps of retinal photoisomerization in proteorhodopsin. *Biophys. J.* 91, 255–262.

(53) Krebs, R. A., Alexiev, U., Partha, R., DeVita, A., and Braiman, M. S. (2002) Detection of fast light-activated H<sup>+</sup> release and M intermediate formation from proteorhodopsin. *BMC Physiol.* 2, 5.

- (54) Xiao, Y. W., Partha, R., Krebs, R., and Braiman, M. (2005) Time-resolved FTIR spectroscopy of the photointermediates involved in fast transient H<sup>+</sup> release by proteorhodopsin. *J. Phys. Chem. B* 109, 634–641.
- (55) Tamogami, J., Kikukawa, T., Miyauchi, S., Muneyuki, E., and Kamo, N. (2009) A tin oxide transparent electrode provides the means for rapid time-resolved pH measurements: Application to photo-induced proton transfer of bacteriorhodopsin and proteorhodopsin. *Photochem. Photobiol.* 85, 578–589.
- (56) Chizhov, I., Chernavskii, D. S., Engelhard, M., Mueller, K.-H., Zubov, B. V., and Hess, B. (1996) Spectrally silent transitions in the bacteriorhodopsin photocycle. *Biophys. J.* 71, 2329–2345.
- (57) Gillbro, T. (1978) Flash kinetic study of the last steps in the photoinduced reaction cycle of bacteriorhodopsin. *Biochim. Biophys. Acta* 504, 175–186.
- (58) Ames, J. B., and Mathies, R. A. (1990) The role of back-reactions and proton uptake during the N → O transition in bacteriorhodopsin's photocycle: A kinetic resonance Raman study. *Biochemistry* 29, 7181–7190.
- (59) Balashov, S. P., Lu, M., Imasheva, E. S., Govindjee, R., Othersen, B., III, Ebrey, T. G., Chen, Y., Crouch, R. K., and Menick, D. R. (1999) The proton release group of bacteriorhodopsin controls the rate of the final step of its photocycle at low pH. *Biochemistry* 38, 2026–2039.
- (60) Brown, L. S., Váró, G., Hatanaka, M., Sasaki, J., Kandori, H., Maeda, A., Friedman, N., Sheves, M., Needleman, R., and Lanyi, J. K. (1995) The complex extracellular domain regulates the deprotonation and reprotonation of the retinal Schiff base during the bacteriorhodopsin photocycle. *Biochemistry* 34, 12903–12911.
- (61) Brown, L. S., Bonet, L., Needleman, R., and Lanyi, J. K. (1993) Estimated acid dissociation constants of the Schiff base, Asp-85, and Arg-82 during the bacteriorhodopsin photocycle. *Biophys. J.* 65, 124–130.
- (62) Dioumaev, A. K., Wang, J. M., Bálint, Z., Váró, G., and Lanyi, J. K. (2003) Proton transport by proteorhodopsin requires that the retinal Schiff base counterion Asp-97 be anionic. *Biochemistry* 42, 6582–6587.
- (63) Sineshchekov, O. A., and Spudich, J. L. (2004) Light-induced intramolecular charge movements in microbial rhodopsins in intact *E. coli* cells. *Photochem. Photobiol. Sci.* 3, 548–554.
- (64) Imasheva, E. S., Balashov, S. P., Wang, J. M., Dioumaev, A. K., and Lanyi, J. K. (2004) Selectivity of retinal photoisomerization in proteorhodopsin is controlled by aspartic acid 227. *Biochemistry* 43, 1648–1655.